Journal of Hazardous Materials 186 (2011) 1355–1359

Contents lists available at ScienceDirect

Journal of Hazardous Materials

journal homepage: www.elsevier.com/locate/jhazmat

Adsorption of fluoride by waste iron oxide: The effects of solution pH, major coexisting anions, and adsorbent calcination temperature

Yao-Hui Huang*, Yu-Jen Shih, Chia-Chi Chang

Department of Chemical Engineering, National Cheng Kung University (NCKU), No. 1 University Rd., Tainan 701, Taiwan

ARTICLE INFO

Article history:
Received 16 September 2010
Received in revised form 6 December 2010
Accepted 6 December 2010
Available online 14 December 2010

Keywords:
Fluidized-bed Fenton
Dehydroxylation
Goethite
Nanopores
Hematite

ABSTRACT

In this study, a waste iron oxide material (BT3), which is a by-product of the fluidized-bed Fenton reaction (FBR-Fenton), was thermally treated between 200 and 900 °C and was used as an efficient adsorbent for the removal of fluoride ions in an aqueous system. The highest fluoride adsorption capacity occurred at the termination of the BT3 goethite dehydroxylation phase at about 300 °C calcination where both the volume of nanopores formed by dehydroxylation and the specific surface area reached their maximum values. Above 300 °C, BT3 transformed to the hematite phase in which fluoride adsorption capacity decreased as calcination temperature increased. On the other hand, the effect of pH on the fluoride adsorption capacity of BT3 for various initial fluoride concentrations was examined. The optimum pH value was found to be about 4. After that efficiency decreased as pH became more alkaline. Finally, coexisting anions affected the fluoride adsorption capacity of BT3 at pH 3.9 ± 0.2 in this order: $PO_4^{3-} > SO_4^{2-} > Cl^- > NO_3^-$.

1. Introduction

Fluoride is known to have both beneficial and detrimental effects on human health. A small amount of the principal mineral constituent, $Ca_5(PO_4)_3F$, can strengthen human teeth (specifically the enamel) and bones. However, prolonged exposure to high levels of fluoride will lead to permanent bone and joint deformations and dental fluorosis [1]. The World Health Organization has set a guidance value of 1.5 mg L^{-1} for fluoride in drinking water [2] (Taiwan's drinking water standard for fluoride is 0.8 mg L^{-1}). Consequently, the treatment of fluoride is an important subject around the world.

Among conventional methods for removing fluoride from water, such as ion exchange, precipitation, and electrolysis, precipitation using chemical agents is the most economical [3]. However the precipitation method requires the use of large amounts of agents, which results in serious problems of sludge disposal. Over the last decade several new treatment methods, such as reverse osmosis, nanofiltration, electrodialysis, and Donnan dialysis, have been proposed in the literature [4–7]. These processes, however, also all have inherent disadvantages that need to be overcome. Many researchers consider adsorption to be the most efficient and applicable technology for fluoride removal from wastewater [8]. Recently, interest in low cost, high surface area metal oxides with distinguished properties has been growing. Numerous researchers have used iron oxide as an adsorbent to treat heavy metals, anions, and hazardous elements in wastewater [9–13].

The iron oxide BT3 is a byproduct of the novel non-seeded FBR-Fenton process where a poorly crystallized goethite phase with extreme purity is derived via Fe^{3+} catalysis. The process not only has high COD removal efficiency, but also reduces a large amount of the Fe sludge produced [14,15]. However, the iron oxide taken out of the FBR-Fenton reactor after an extended reaction is a waste product. In our previous studies, iron oxide BT3 was used for treating wastewater from leather plants in Taiwan. We successfully applied BT3 as an adsorbent for the removal of copper (Cu^{2+}) and lead (Pb^{2+}) from aqueous solutions [11,13]. Furthermore, the Langmuir and Freundlich equations have been used to evaluate the thermodynamics and kinetics of the F^- adsorption of the BT3 adsorbent [16]. This absorbent has been found to be a prominent material, which could provide economical and efficient fluoride removal.

The effect of calcination at various temperatures on single adsorbents being used for fluoride adsorption is seldom discussed in the literature. In this study, iron oxide BT3 adsorbent is thermally treated for testing the relationship between the specific surface area that is thermally changed and fluoride removal efficiency in aqueous solutions. The influences of pH and species of coexisting anions on adsorption capacity are also investigated.

2. Materials and methods

2.1. Materials

The BT3 adsorbent used for F^- adsorption in this study was obtained using the following procedure [17]: iron oxide was packed as a carrier in a 25 m^3 (1.9 m-Φ × 9 m-H) FBR-Fenton reactor in a

* Corresponding author. Tel.: +886 6 2757575x62636; fax: +886 6 2344496.
E-mail address: yhhuang@mail.ncku.edu.tw (Y.-H. Huang).

0304-3894/$ – see front matter © 2010 Elsevier B.V. All rights reserved.
doi:10.1016/j.jhazmat.2010.12.025

Table 1
BET surface area and pore characteristics of BT3 calcined at various temperatures.

	BT3	Calcination temperature							
		200	300	400	500	600	700	800	900
Surface area (m^2/g)	105.0	109.3	124.7	116.8	59.7	39.5	15.7	7.2	2.1
Pore vol. (cm^3/g)	0.04	0.06	0.13	0.12	0.10	0.16	0.16	0.17	0.17

wastewater treatment plant. By controlling the internal circulation, the superficial up flow velocity was maintained at 40 m/h with a 50% bed expansion. H_2O_2 (Union Chemical) and $FeSO_4$ (technical grade) with a molar ratio of 2:1 were fed into the reactor bottom continuously. The pH of the solution was controlled at 3.5 to prevent $Fe(OH)_3$ precipitation. The BT3, a poorly crystallized goethite phase, was then homogeneously nucleated to be a by-product of the FBR-Fenton reaction. An aqueous stock solution of sodium fluoride (NaF, Riedel-de Haen) was prepared using deionized water (Millipore Milli-Q) to simulate the F^--contaminated wastewater.

2.2. Methods

The iron oxide-BT3 sample collected from the FBR-Fenton reaction was heated at various calcination temperatures. The pore size distribution and specific surface area of calcined BT3 were then determined using the N_2 adsorption–desorption method. A structural and thermal analysis was performed to characterize the phase transition of the BT3 using a powder diffractometer (Rigaku RX III) with Cu Ka radiation and DTA/TG.

1 g/L of BT3 adsorbent was added to each of the various solutions with various initial F^- concentrations. These samples were then mounted on the Jar Test apparatus for 48 h at room temperature. The solutions' pH levels were controlled by adding dilute HNO_3 or NaOH solutions throughout the experiment. The suspensions were filtered using a 0.45 mm syringe filter made of poly-(vinylidene fluoride) membrane, and the filtrates were immediately measured using ion-exclusion chromatography with a 4.6 mm ID_250 mmL Metrosep A SUPP 1 column (Metrohm, USA). The adsorption capacity was determined as the difference between the initial and the equilibrium F^- concentrations.

3. Results and discussion

3.1. Characterization

The BET specific surface areas and pore volumes of the 200–900 °C thermally treated BT3's are presented in Table 1. Obviously, the specific surface area of BT3 is significantly changed by calcination. As the temperature was increased from room temperature up to 300 °C, the BET surface area increased from 105.0 m^2/g to 124.7 m^2/g, and was accompanied by an increase in the pore volume. Calcination above 300 °C resulted in a decrease in the specific surface area due to grain coarsening. Fig. 1 reveals the DTA/TG thermal analysis of BT3. The thermal event associated with the transformation from goethite to hematite is exothermic, as given in Fig. 1 (at 261 °C) and in [18]:

$$2FeOOH \rightarrow \alpha\text{-}Fe_2O_3 + H_2O \quad (1)$$

The dehydroxylation reaction accompanying the goethite–hematite transformation was observed through XRD (Fig. 2). The original BT3 was a poorly crystallized goethite (FeOOH) phase, which is characterized by the broadening of XRD lines, and its transformation to the poorly crystallized hematite (α-Fe_2O_3) phase at 300 °C alludes to the result of the DTA/TG analysis. As calcination temperatures increased from 300 to 900 °C, diffraction peaks gradually sharpened, which suggest that this phase converts into well-crystallized hematite at about 700 °C.

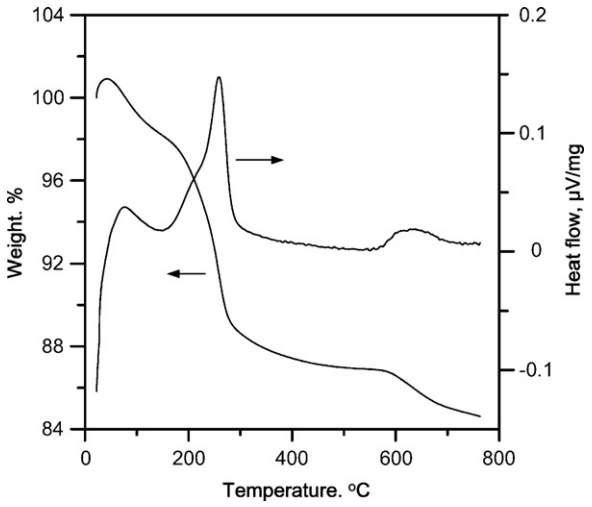

Fig. 1. DTA/TG analysis of the BT3 sample.

Porosity is one of the characteristics observed as a result of the loss of water in the dehydroxylation reaction [19,20]. There is no measurable porosity in the original BT3 as shown in Fig. 3. Calcination up to 300 °C results in the formation of nanopores. From 300 to 600 °C, the pore volume increases while the specific surface area decreases from 124.7 m^2/g to 39.5 m^2/g. According to the pore size distribution, the thermal-induced atomic diffusion causes the nanopores to penetrate out and assemble into larger pores, leading to a decrease in surface area.

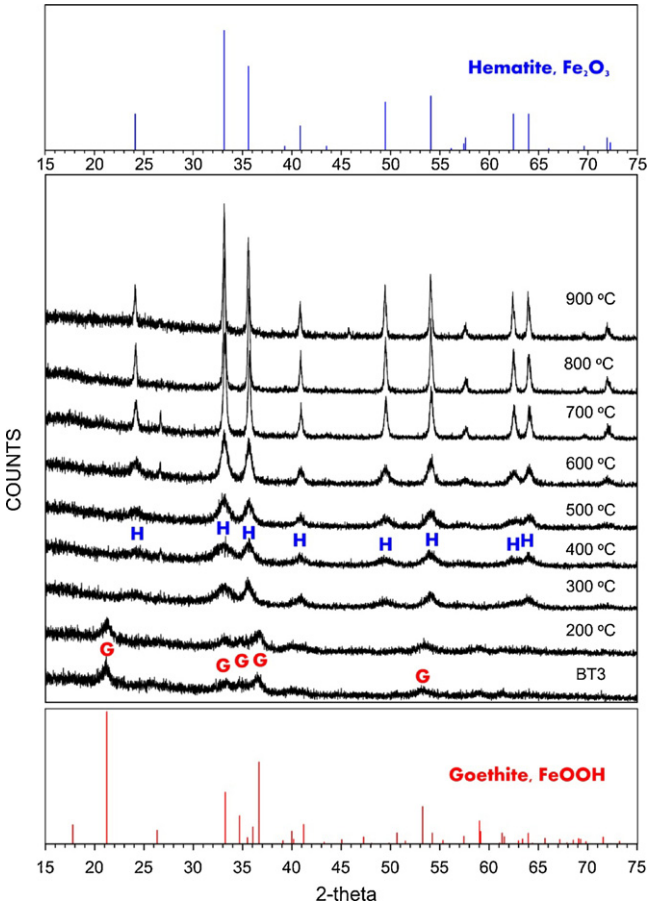

Fig. 2. X-ray diffraction patterns of BT3 and 200–900 °C calcined samples.

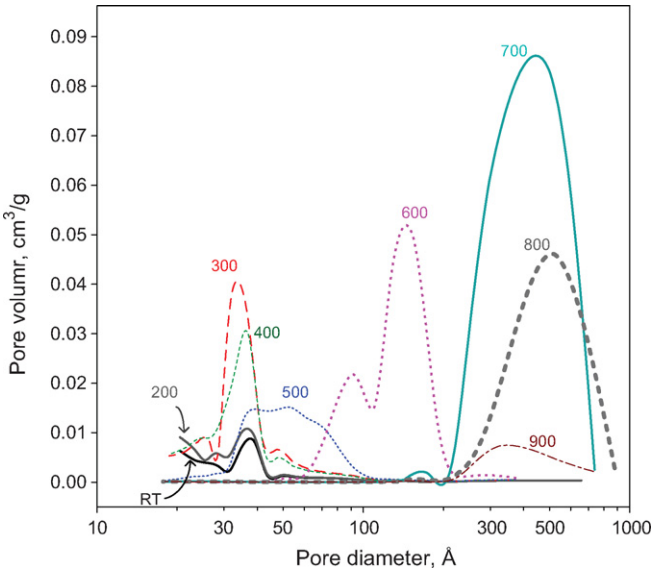

Fig. 3. Pore size distribution of BT3 and 200–900 °C calcined samples.

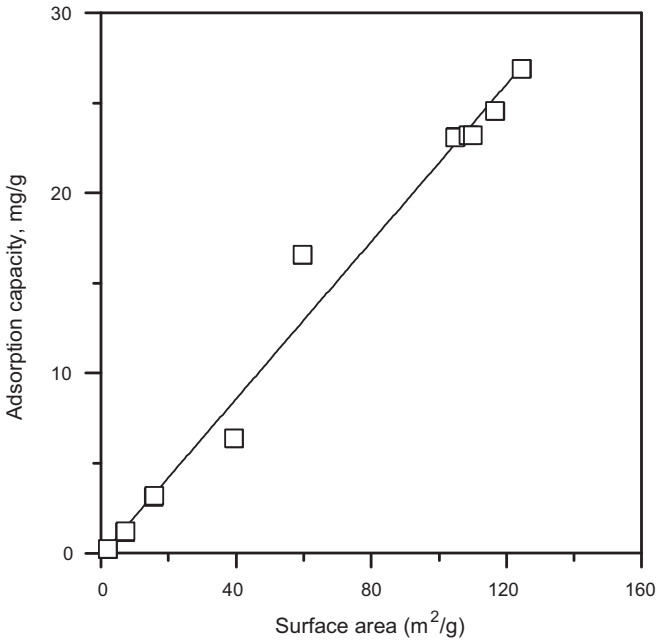

Fig. 5. Relationship between fluoride adsorption capacity and BET surface area of BT3. (Initial conc.: 6 mM, solid loading: 1 g L^{-1}, pH = 4.)

3.2. Effect of calcination temperature of BT3 on fluoride adsorption

The slight increase in the adsorption capacity of the calcined BT3 coincided with the threshold of the dehydroxylation (~200 °C) (Fig. 4). The maximum of adsorption capacity, 27 mg/g, occurred at about the same time as the termination of dehydroxylation (Fig. 1), when the calcination temperature reached about 300 °C. It is rational to believe that the number of adsorption sites for fluoride depends on the surface area and on the nature of the surface. The number of adsorption sites increases correlatively with the formation of nanopores when FeOOH transforms to α-Fe_2O_3. Above 300 °C, a shrinkage of nanopores occurs (Fig. 3) and is accompanied by the decrease of the specific surface area (Table 1) and of the number of adsorption sites. Similar results were reported by Mandal and Mayadevi [21] for the adsorption of fluoride in Zn–Al LDHs.

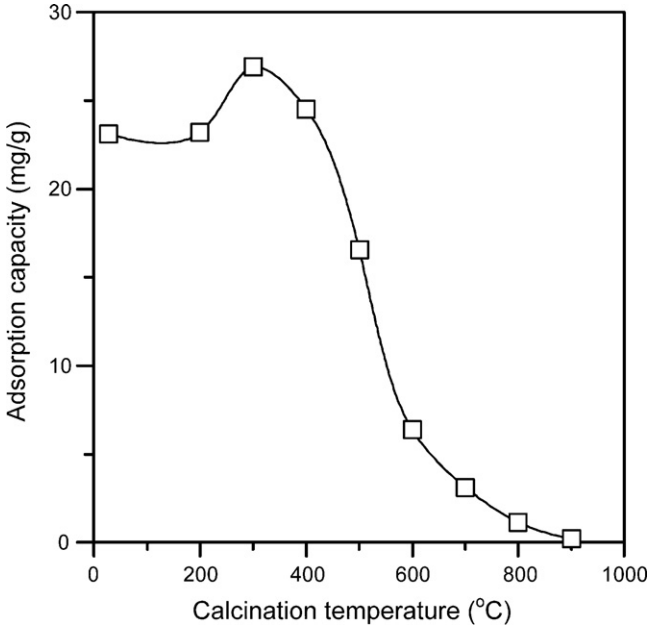

Fig. 4. Effect of calcination temperature on fluoride adsorption of BT3. (Initial conc.: 6 mM, solid loading: 1 g L^{-1}, pH = 4.)

The adsorption capacity depends on the surface area (measured using the BET method). We observed a positive relationship between them. The results of this fitting data are shown in Fig. 5. The coefficient for the linear method's r^2 was 0.98. The fluoride adsorption capacity increased very linearly with BET surface area. Similar results were found by Batzias et al. [22] who used acid hydrolyzed lignocellulosic material to enhance the exhibition of advanced adsorption properties and found that the BET surface area increased linearly with the percentage of removed polysaccharides.

3.3. Effects of pH and coexisting anions on the fluoride adsorption

The most important factor that controls the adsorption of ions on the oxide surface is the pH of the aqueous solution. Since anion adsorption is coupled with a release of OH^- ion, the adsorption of the fluoride on the BT3 surface is probably favored at low pH values. The specific adsorption of fluoride on metal oxide was modeled as a two-step ligand-exchange reaction [23]:

$$SOH + H^+ \rightarrow SOH_2^+ \quad (2)$$

$$SOH_2^+ + F^- \rightarrow SF + H_2O \quad (3)$$

which combined gives

$$SOH + H^+ + F^- \rightarrow SF + H_2O \quad (4)$$

where S represents the exposed metal ion of the adsorbent.

Fig. 6 shows the effects of pH on the fluoride adsorption capacity of BT3 using 1.5, 3, and 6 mM initial fluoride concentrations. The pH values ranged from 2 to 12. The adsorption capacity of BT3 shows a similar tendency, which rises with increases in the initial fluoride concentration. The adsorption of fluoride increases in the acidic pH range and reaches a maximum near pH 4, and then decreases as pH increases. The maximum adsorption capacity for 1.5, 3, and 6 mM initial fluoride concentrations were 12.0, 17.3, and 20.4 mg/g, respectively. The lower fluoride adsorption of BT3 below pH 4 may be attributed to the competition between adsorption behavior and the formation of hydrofluoric acid. According to the fluoride spe-

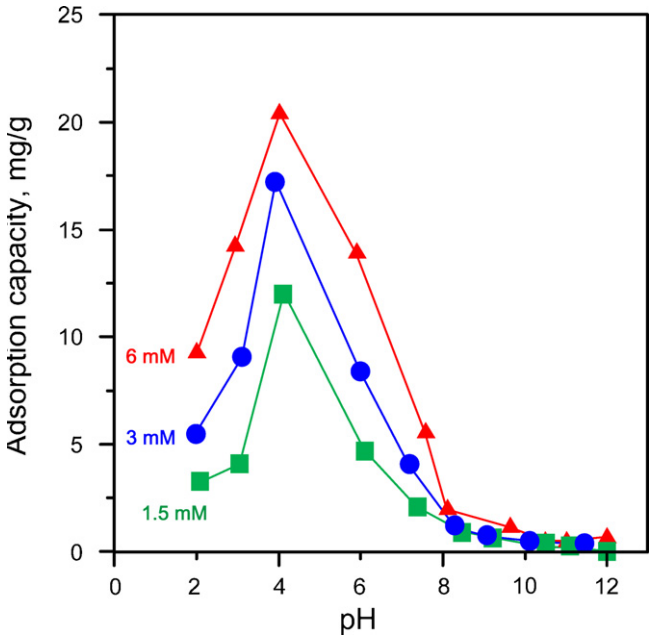

Fig. 6. Effect of pH on fluoride removal using BT3 (solid loading: 1 g L^{-1}) for various initial fluoride concentrations.

ciation, hydrofluoride was predominant in pH condition less than 3.18 [24].

The surface potential theory suggests that the sharp decrease in fluoride adsorption above pH 4 may be due to the decrease in surface charges of BT3 at varying pH values [25]. The pH_{zpc} of BT3 tested in our previous study was about 4.10 [16]. Above pH_{zpc}, the iron oxide surface became negative charged. The surface charge hinders fluoride adsorption but never eliminates fluoride removal until the pH values are increased to 8, where capacities hover below 2 mg/g. In other words, electrostatic adsorption was probably not the main mechanism causing fluoride transfer to the BT3.

A variety of anions are generally present in fluoridated water. In this study, the effects of PO_4^{3-}, SO_4^{2-}, Cl^- and NO_3^- were examined at pH = 3.9 ± 0.2. The initial concentration of fluoride was 6 mM in all experiments, whereas concentrations of other anions varied from 0.6 to 60 mM. Fig. 7 shows that the fluoride adsorption ratio decreased from 99 to 18% when the PO_4^{3-} concentration was increased from 0 to 60 mM. Fluoride adsorption also decreased substantially when sulfate was present in the system. Cl^- and NO_3^- had less impact on fluoride adsorption, as compared to sulfate tests. Cl^- and NO_3^- are low-affinity ligands. Their adsorption mechanism occurs via weaker bonds of outer-sphere complexation with the active sites, while SO_4^{2-} forms both outer-sphere and inner sphere complexes with the active sites in aqueous systems [26]. Therefore, the depression of coexisting anions on fluoride adsorption follows this order: $PO_4^{3-} > SO_4^{2-} > Cl^- > NO_3^-$. This indicates that anions with lower ionic potentials tend to be less preferably adsorbed by BT3, and also reflects the relatively competitive and inhibitive effects of these anions on the fluoride adsorption of BT3 [27,28].

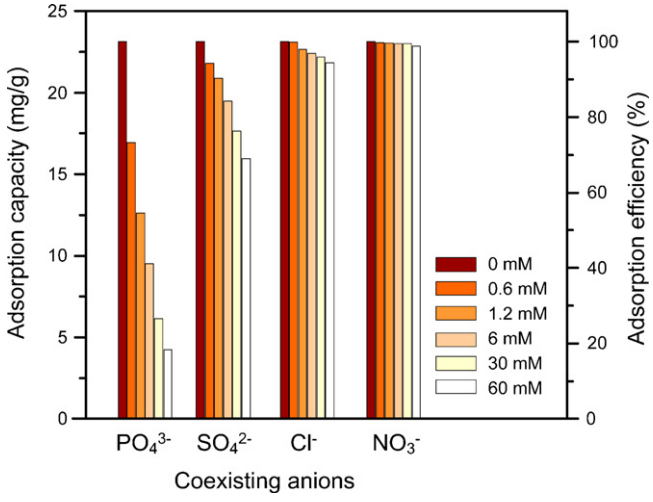

Fig. 7. Effects of co-existing anions on fluoride removal. (Initial fluoride conc.: 6 mM, pH: 3.9 ± 0.2, solid loading: 1 g L^{-1}.)

4. Conclusions

Continuing our previous work [15], we investigated in this study the effects of the calcination of BT3 iron oxides on fluoride adsorption capacity. Before the transformation to hematite was fully achieved, the dehydroxylation of goethite–BT3 left nanopores and enhanced the fluoride adsorption capacity. When the calcination temperature was increased from 300 to 900 °C, the transition of poorly to well-crystallized hematite phase dominated. Then, the adsorption capacity decreased with the specific surface area; this is probably due to the shrinkage of the nanopores into larger ones. Furthermore, the fluoride adsorption capacity of BT3 varied with different pH values and reached a maximum at about pH 4. The maximum of capacity increased from 12.0 mg/g to 20.4 mg/g as the initial fluoride concentration increased from 1.5 mM to 6.0 mM. The adsorption capacity of BT3 decayed above pH 4, where the iron oxide surface inverted from a positive to a negative charge, suggesting that the adsorption mechanism is substantially hindered by electrostatic force. Finally, the effect of coexisting anions was examined using PO_4^{3-}, SO_4^{2-}, Cl^- and NO_3^- at pH = 3.9 ± 0.2. The anions ability to hinder BT3's fluoride adsorption followed this order: $PO_4^{3-} > SO_4^{2-} > Cl^- > NO_3^-$.

References

[1] M. Mohapatra, S. Anand, B.K. Mishra, D.E. Giles, P. Singh, Review of fluoride removal from drinking water, J. Environ. Manag. 91 (2009) 67–77.
[2] WHO, Chemical fact sheets: fluoride. In: Guidelines for Drinking Water Quality (electronic resource): Incorporation First Addendum, third ed., Recommendations, Geneva, 2006.
[3] C.L. Yang, R. Dluhy, Electrochemical generation of aluminum sorbent for fluoride adsorption, J. Hazard. Mater. 94 (2002) 239–252.
[4] M. Hichour, F. Persin, J. Sandeaux, C. Gavach, Fluoride removal from water by Donnan dialysis, Sep. Purif. Technol. 18 (2000) 1–11.
[5] Z. Amor, B. Bariou, N. Mameri, M. Taky, S. Nicolas, A. Elmidaoui, Fluoride removal from brackish water by electrodialysis, Desalination 133 (2001) 215–223.
[6] H. Garmes, F. Persin, J. Sandeaux, G. Pourcelly, M. Mountadar, Defluoridation of groundwater by a hybrid process combining adsorption and Donnan dialysis, Desalination 145 (2002) 287–291.
[7] H. Mjengera, G. Mkongo, Appropriate defluoridation technology for use in fluorotic areas in Tanzania, Phys. Chem. Earth 28 (2003) 1097–1104.
[8] T. Hiemstra, W.H. Van Riemsdijk, Fluoride adsorption on goethite in relation to different types of surfaces sites, J. Colloid Interface Sci. 225 (2000) 94–104.
[9] M.P. Asta, J. Cama, M. Martinez, J. Gimenez, Arsenic removal by goethite and jarosite in acidic conditions and its environmental implications, J. Hazard. Mater. 171 (2009) 965–972.
[10] Y.J. Wang, D.M. Zhou, R.J. Sun, D.A. Jia, H.W. Zhu, S.Q. Wang, Zinc adsorption on goethite as affected by glyphosate, J. Hazard. Mater. 151 (2008) 179–184.
[11] Y.-H. Huang, C.-L. Hsueh, H.-P. Cheng, L.-C. Su, C.-Y. Chen, Thermodynamics and kinetics of adsorption of Cu(II) onto waste iron oxide, J. Hazard. Mater. 144 (2007) 406–411.
[12] P. Lakshmipathiraj, B.R.V. Narasimhan, S. Prabhakar, G.B. Raju, Adsorption of arsenate on synthetic goethite from aqueous solutions, J. Hazard. Mater. B 136 (2006) 281–287.
[13] A. Iglesias, R. López, D. Gondar, J. Antelo, S. Fiol, F. Arce, Adsorption of paraquat on goethite and humic acid-coated goethite, J. Hazard. Mater. (2010) (available online 26 July).
[14] S. Chou, C. Huang, Y.-H. Huang, Effect of Fe^{2+} on catalytic oxidation in a fluidized bed reactor, Chemosphere 39 (1999) 1997–2006.

[15] S. Chou, C. Huang, Y.H. Huang, Heterogeneous and homogeneous catalytic oxidation by supported γ-FeOOH in a fluidized-bed reactor: kinetic approach, Environ. Sci. Technol. 35 (2001) 1247–1251.
[16] C.C. Chang, Y.H. Huang, H.T. Chan, Adsorption thermodynamic and kinetic studies of fluoride aqueous solutions treated with waste iron oxide, Sep. Sci. Technol. 45 (2010) 370–379.
[17] Y.H. Huang, G.H. Huang, S.S. Chou, H.S. You, S.H. Perng, Process for chemically oxidizing wastewater with reduced sludge production, United States Patent 6,143,182. (2000).
[18] R. Derie, M. Ghodsi, C. Calvo-Roche, DTA study of the dehydration of synthetic goethite α-FeOOH, J. Therm. Anal. 9 (1976) 435–440.
[19] A.F. Gualtieri, P. Venturell, In situ study of the goethite–hematite phase transformation by real time synchrotron powder diffraction, Am. Mineral. 84 (1999) 895–904.
[20] P.S.R. Prasada, K.S. Prasada, V.K. Chaitanya, E.V.S.S.K. Babu, B. Sreedhar, S.R. Murthyd, In situ FTIR study on the dehydration of natural goethite, J. Asian Earth Sci. 27 (2006) 503–511.
[21] S. Mandal, S. Mayadevi, Adsorption of fluoride ions by Zn–Al layered double hydroxides, Appl. Clay Sci. 40 (2008) 54–62.
[22] F. Batzias, D. Sidiras, E. Schroeder, C. Weber, Simulation of dye adsorption on hydrolyzed wheat straw in batch and fixed-bed systems, Chem. Eng. J. 148 (2009) 459–472.
[23] S.S. Tripathy, J.-L. Bersillon, K. Gopal, Removal of fluoride from drinking water by adsorption onto alum-impregnated activated alumina, Sep. Purif. Technol. 50 (3) (2006) 310–317.
[24] W. Stumm, J.J. Morgan, Aquatic Chemistry, 3rd ed., John Wiley & Sons, Inc., 1996, pp. 533–549.
[25] A. Barnes, D.J. Sapsford, M. Dey, K.P. Williams, Heterogeneous Fe(II) oxidation and zeta potential, J. Geochem. Explor. 100 (2009) 192–198.
[26] A. Eskandarpour, M.S. Onyango, A. Ochieng, S. Asai, Removal of fluoride ions from aqueous solution at a low pH using schwertmannite, J. Hazard. Mater. 152 (2008) 571–579.
[27] Y. Tang, X. Guan, J. Wang, N. Gao, M.R. McPhail, C.C. Chusuei, Fluoride adsorption onto granular ferric hydroxide: effects of ionic strength, pH, surface loading, and major co-existing anions, J. Hazard. Mater. 171 (2009) 774–779.
[28] Kok-Hui Goh, Teik-Thye Lim, Influences of co-existing species on the sorption of toxic oxyanions from aqueous solutions by nanocrystalline Mg/Al layered double hydroxide, J. Hazard. Mater. 180 (2010) 401–408.